TESLA - COLLABORATION

Single Bunch Energy Spread in the TESLA Cryomodule

A. Novokhatski, M. Timm, T. Weiland

TH Darmstadt

September 1999, TESLA 99-16

TESLA Reports are available from:

Deutsches Elektronen-Synchrotron DESY
MHF-SL Group
Katrin Lando
D-22603 Hamburg
Germany

Phone: (+49/40) 8998 3339
Fax: (+49-40) 8998 4302
e-mail: katrin.lando@desy.de

http://tesla.desy.de/new_pages/TESLA/TTFnotes.html

Single Bunch Energy Spread in the TESLA Cryomodule

Alexandre Novokhatski, Martin Timm and Thomas Weiland

Fachgebiet Theorie Elektromagnetischer Felder
Technische Universität Darmstadt
Schloßgartenstraße 8, D-64289, Darmstadt

September 2, 1999

Abstract

The beam energy spread in a linear accelerator is determined by the accelerating field of an external generator and the wake fields, excited by the beam in the accelerating structure. The single bunch energy spread strongly depends upon the bunch length, and the shape of the charge distribution.

In this paper we present formulas for the RMS energy spread calculation. Four integral parameters of the wake field are found to be sufficient for the calculation of the RMS energy spread of a Gaussian bunch.

Wake fields in a TESLA accelerating cryomodule and corresponding integral parameters are given for bunches of different length.

The relative energy spread can be decreased several times by shifting the bunch injection phase to some optimum value, naturally with a decrease energy gain. Minimum energy spread, optimal phases and energy gain are tabulated for different bunch parameters, proposed for TTF-2, TTF-FEL, TESLA-500, TESLA-800 and TESLA-FEL.

1 Introduction

The beam energy spread is a very important parameter for new projects of Linear Colliders and X-ray Free Electron Lasers [1]. In the linear accelerator it is determined by the accelerating field of an external generator and by the wake fields, excited by the beam in the accelerating structure. The single bunch energy spread strongly depends upon both, the bunch length and the shape of the charge distribution.

The field of the external generator has a simple, analytical description. However for the wake field calculations we have to solve Maxwell equations for a given current in an accelerating structure [5], [6]. The interaction region between the bunch and the wake fields is very long for very short bunches [7], [8]. For this reason, the fields calculated for a cell or a cavity with initial condition of an infinite tube cannot be taken and then be simply summed up in order to obtain the total field. A full wake field calculation has to be carried out along a considerable length of accelerating structure until the accompanying bunch field reaches the "steady-state" distribution. Naturally we have to include in the calculations all structure elements, like variation of the cross section of the vacuum chamber, bellows, etc.

In this paper a simple analytical formula for the RMS energy spread is derived, using only four integral parameters of the wake field, under the assumption, that the bunch in the linear accelerator has Gaussian charge density distribution.

Tables for the minimum energy spread, the optimal phase and the energy spread are given for the parameter sets of

TESLA-CDR [1]	($\sigma = 700\mu$m, Q=5.8nC),
TESLA-500 high Luminosity [2]	($\sigma = 400\mu$m, Q=3.2nC),
TESLA-800 [2]	($\sigma = 300\mu$m, Q=2.24nC),
TESLA-FEL [1]	($\sigma = 50\mu$m, Q=1nC).

The studied parameter sets for the TESLA Test Facility are

TTF-2 [3]	($\sigma = 1$mm, Q=8nC),
TTF-FEL [4]	($\sigma = 250\mu$m, Q=1nC).

2 Wake fields in the TESLA accelerating structure

The TESLA accelerating structure is a set of super conductive cryomodules. Each accelerating cryomodule consists of eight cavities, separated by drift tubes with bellows. There are two more bellows at the beginning and the end of every cryomodule (Fig.1). Each cryomodule cavity contains seven regular cells with the aperture of 35mm and two end cells with the aperture of the drift tube, which is 39mm.

One cryomodule is chosen to be the main element for the wake field calculation for TTF-2, TTF-FEL, TESLA-500 and TESLA-800 parameters. In Fig.2 and Fig.3 the wake fields of 700 μm and 300 μm bunch are shown.

The length of one cryomodule ($\approx 10m$) is enough for the wake field of a $200\mu m$ bunch to come to the "steady-state quasi periodic solution". As an example the development of the wake field of a $250\mu m$ bunch inside a TESLA cryomodule is shown (Fig.4). For shorter bunches we have to carry out wake field calculation in two or even more cryomodules. This is demonstrated for a 50 μm bunch. The wake fields in two consecutive TESLA cryomodules, separated by a long drift tube are presented(Fig.5).

The wake fields of the bunches of other length and an analytical approximation thereof are presented in the next chapter.

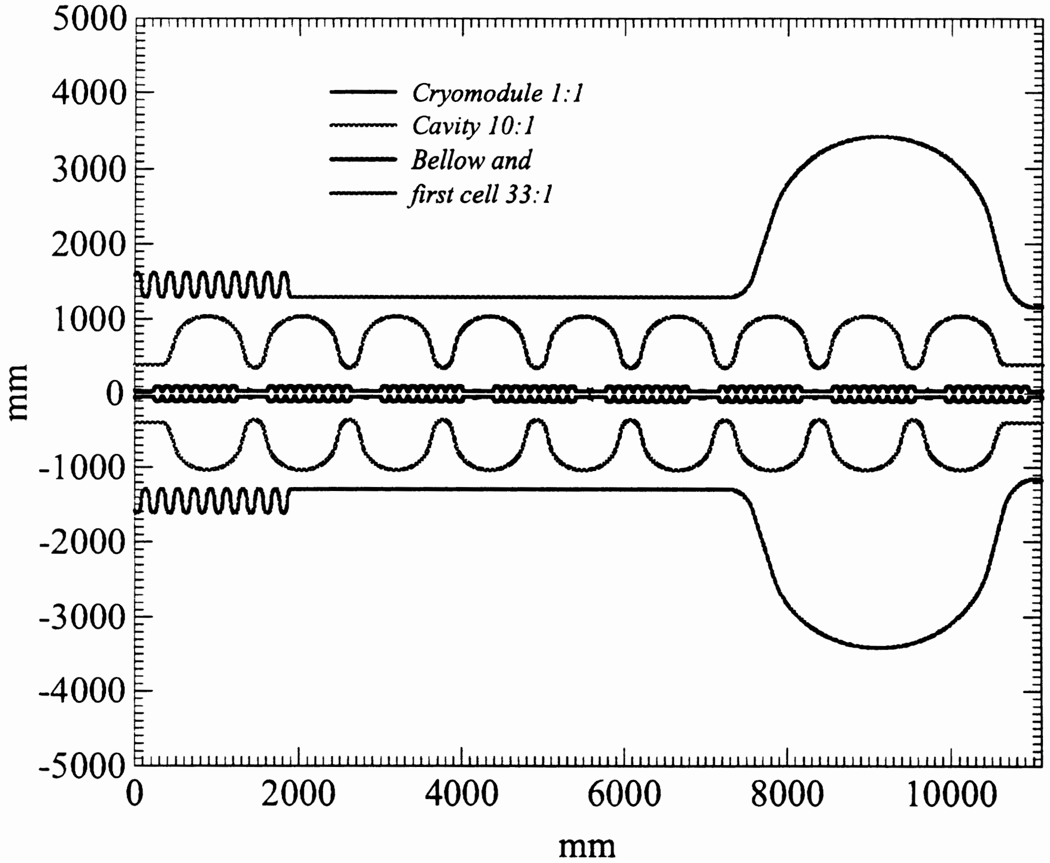

Figure 1: TESLA cryomodule, cavity, bellow and end cell.

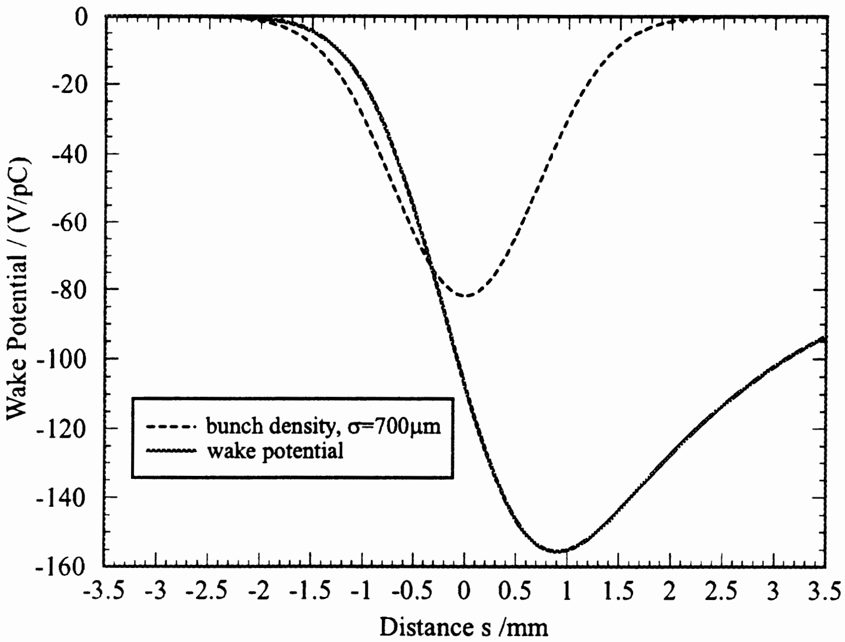

Figure 2: Wake potential for a bunch length of $\sigma = 700\mu$m due to a TESLA cryomodule.

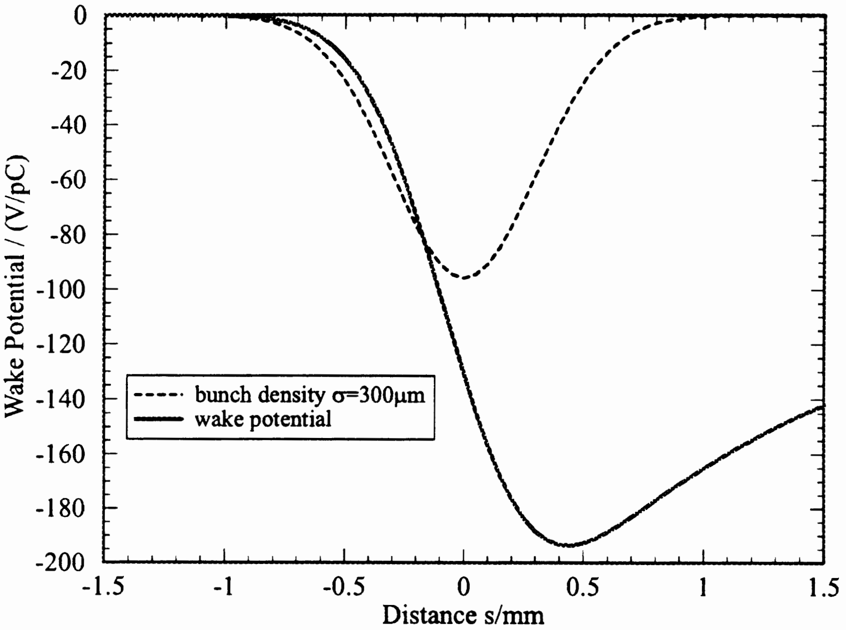

Figure 3: Wake potential for a bunch length of $\sigma = 300\mu$m due to a TESLA cryomodule.

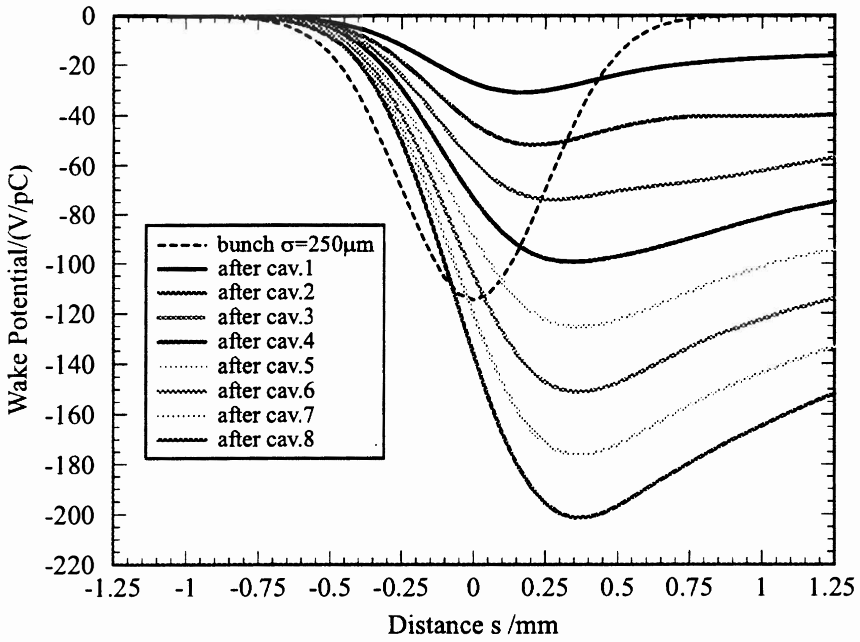

Figure 4: Wake potential development for a bunch length of $\sigma = 250\mu$m due to a TESLA cryomodule.

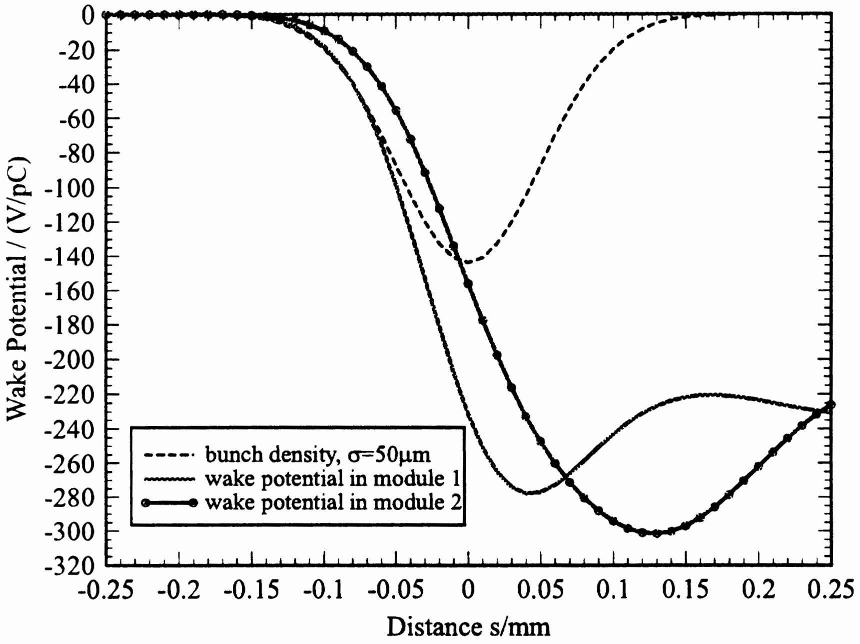

Figure 5: Wake potential for a bunch length of $\sigma = 50\mu$m bunch due to two consecutive TESLA cryomodules separated by a drift tube of 7λ length.

3 Analytical approximation of the wake potential of the TESLA accelerating structure

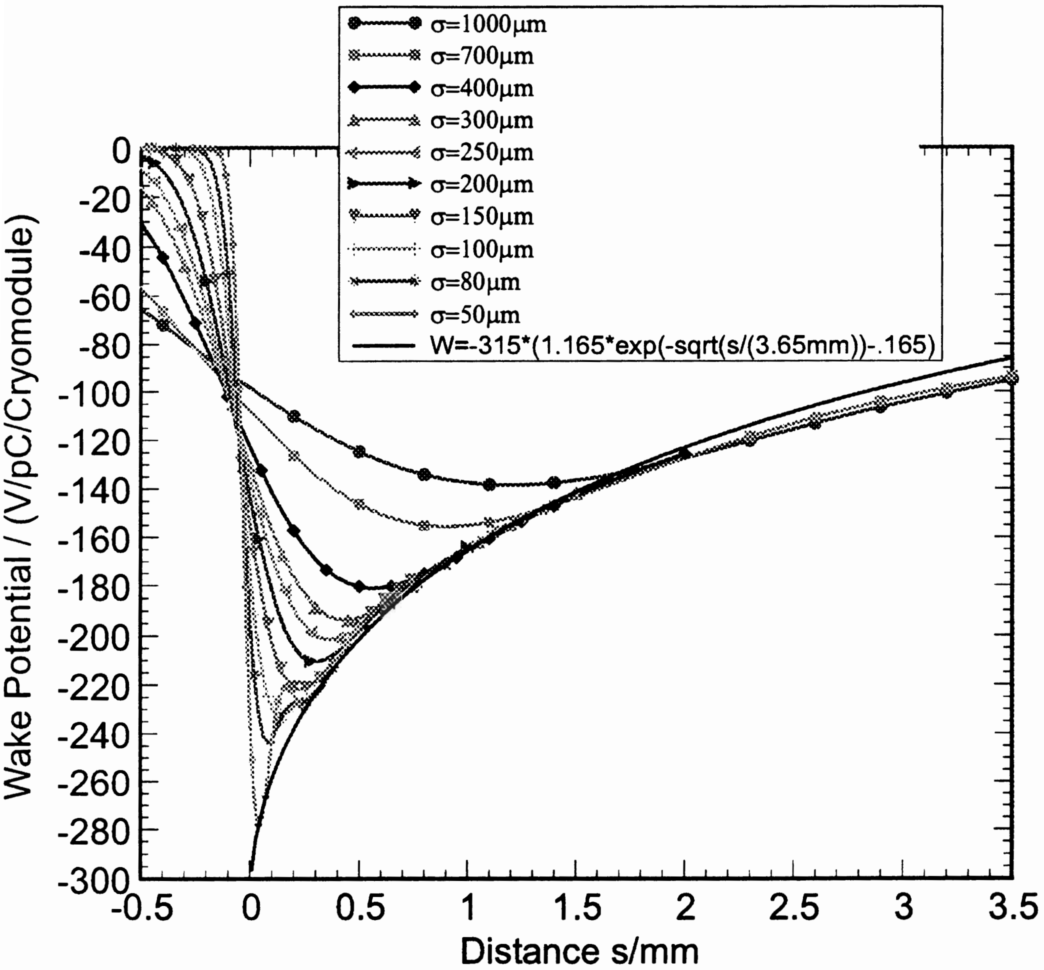

Figure 6: Wake fields of bunches of different length in a TESLA cryomodule. The approximation of the wake function (Eq. 3) is shown as well.

The wake fields of Gaussian shaped bunches with different length in the TESLA accelerating structure (Fig.1), resulting from numerical time domain simulations, are plotted together on Figure 6. As the bunch length decreases, the amplitude of the wake field increases. After a certain distance to the bunch centre, approximately twice the bunch length, the wake fields follow a common curvature. This curve is smooth and monotonic from approximately

300μm on (Fig. 6).

The long range wake field of a bunch with $\sigma = 1000\mu$m (Fig.8) starts reflecting some geometrical properties of the structure at a distance of 20mm to the bunch head. In the smooth region between 300μm and 20mm the wake field is determined mainly by the iris radius.

The enveloppe function, common to all wake fields (Fig. 6), tends to be the wake potential of a point charge. Convolution with the charge distribution of the bunch gives the wake field

$$W(s) = \frac{1}{Q} \int_{-\infty}^{s} w(s - s')q(s')ds'. \tag{1}$$

The analytical expression [7]

$$w(s) = A_0 \frac{Z_0 c}{\pi a^2} \left((1 + \beta_0) \exp\left(\sqrt{\alpha_0 \frac{s}{s_0}} \right) - \beta_0 \right) \tag{2}$$

is used to approximate the wake function. Here Z_0 is the impedance of free space, c is the speed of light. A_0, β_0 and α_0 are fitting parameters. A_0 and α_0 are in the order of 1 and $\beta_0 << 1$.

Fitting the parameters of Eq. 2 to the results of the numerical simulation yields the wake potential per cryomodule

$$w(s) = 315 \left[\frac{\mathrm{V}}{\mathrm{pC}} \right] \left(1.165 \cdot \exp\left(\sqrt{\frac{s}{3.65\mathrm{mm}}} \right) - 0.165 \right). \tag{3}$$

Results of wake potentials derived by this this approximation for bunches with Gaussian charge distribution and different length — $\sigma = 700\mu$m for *TESLA-CDR*, $\sigma = 400\mu$m for *TESLA-500 High Luminosity* for *TESLA-CDR* — are displayed on Fig. 7.

The comparison between this approximation of the wake potential and the results of the numerical simulation shows (Fig. 7), that for the the bunches with $\sigma = 700\mu$m and $\sigma = 400\mu$m a good agreement is found. In case of the $\sigma = 50\mu$m bunch the steady state solution is not reached, even after two consecutive cryomodules, although the slope of the analytical approximation comes closer to the transient wake potential after the second cryomodule.

The approximated wake potential (Eq. 3), in turn, is plotted together with the wake fields, derived form the numerical simulations (Fig. 6). Its course approximates the envelope function of the wake potential too.

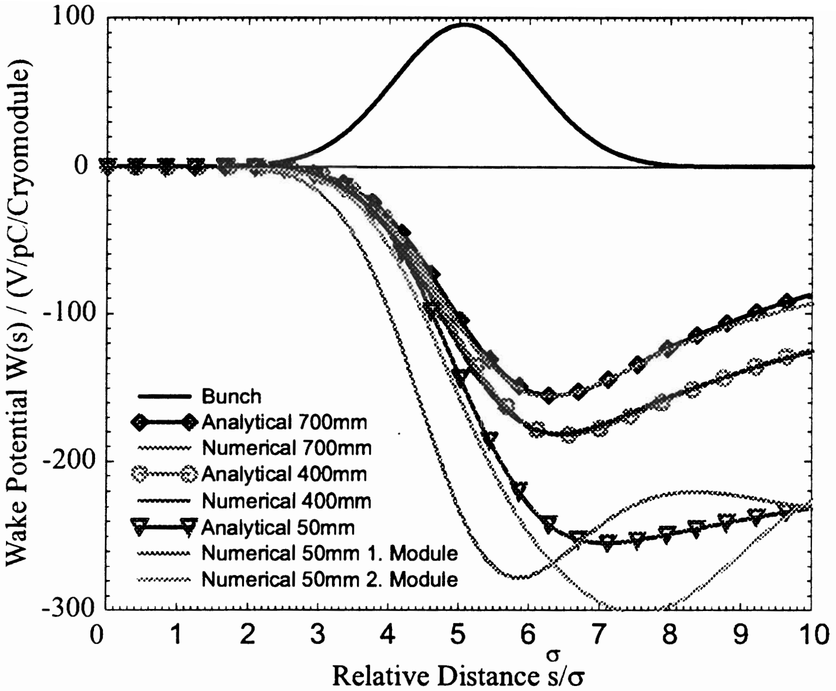

Figure 7: Comparison of the wake potentials of a bunch inside a TESLA cryomodule calculated by numerical simulation and by convolution of the analytical formula (Eq. 3) for $\sigma = 700\mu$m, 400μm and 50μm.

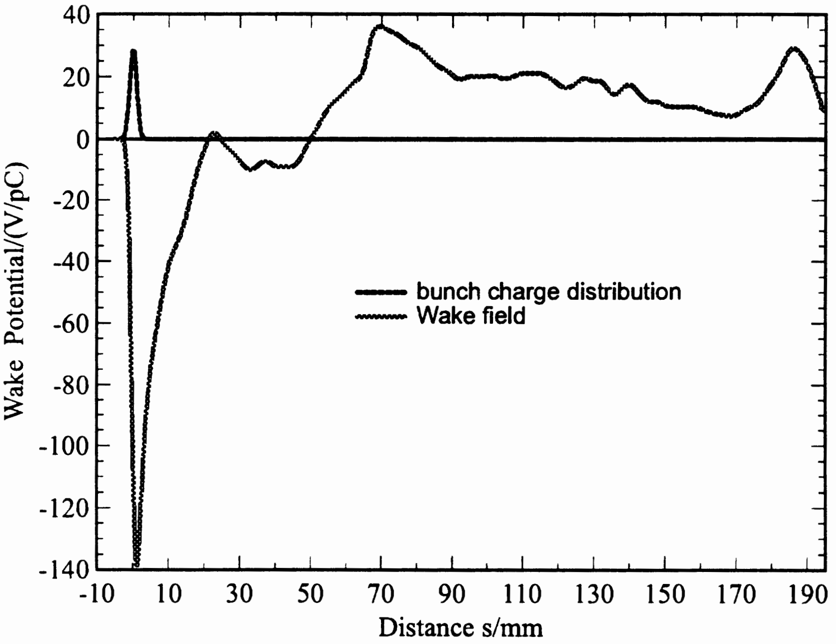

Figure 8: Long range wake potential of a $\sigma = 1$mm bunch after the passage of a TESLA cryomodule

4 Energy spread and Integral parameters of the Wake fields

The bunch, travelling through the accelerating structure, is considered to have the Gaussian charge density distribution $q(s)$

$$q(s) = \frac{Q}{\sqrt{2\pi}\sigma} e^{-s^2/2\sigma^2}$$

with the bunch length σ. It is carrying the total charge Q.

Assuming that the initial energy and the energy spread are small – compared to that gained from the accelerating structure – a particle with a distance s from the center of the bunch, gains the energy $U(s)$. This is the sum of the energy gain from the field of the external generator E_{ac} and the energy loss (or gain) due to the wake fields E_w

$$U(s) = e \int (E_{ac}(t,z) + E_w(t,z))_{t=\frac{z-s}{c}} dz = U_0 \cdot V(s) + Q \cdot W(s),$$

where U_0 is the maximum energy gain in the structure due to the external generator only. The energy gain per unit voltage from the external generator can be written as

$$V(s) = \cos(ks + \phi),$$

where $\omega = kc$ is the angular frequency of the accelerating field and ϕ is the phase of injection, relative to the phase of the maximum energy gain.

The particles energy loss (or energy exchange inside the bunch) is described by the wake potential $W(s)$. The average value of the total energy change $\langle U \rangle$ is the sum of the average gains due to the accelerating field and the wake potentials

$$\langle U \rangle = \int_{-\infty}^{+\infty} U(s) q(s) ds = U_0 \cdot \langle V \rangle + Q \cdot \langle W \rangle,$$

where

$$\langle V \rangle = \cos(\phi) e^{-(k\sigma)^2/2}, \qquad \langle W \rangle = K_\sigma.$$

K_σ is the loss factor of a bunch with a unit charge [1]. It has the negative value

---

[1] As we usually measure the loss factor in [V/pC], we have to measure the charge Q in [pC].

$$K_\sigma = \frac{1}{Q}\int_{-\infty}^{+\infty} q(s)W(s)ds. \tag{4}$$

The average squared energy spread $\langle \Delta U^2 \rangle$ of the bunch is

$$\langle \Delta U^2 \rangle = \langle [U(s) - \langle U \rangle]^2 \rangle.$$

Transforming this equation yields

$$\langle \Delta U^2 \rangle = U_0^2 \cdot \langle \Delta V^2 \rangle + Q^2 \cdot \langle \Delta W^2 \rangle + 2U_0 Q \cdot [\langle V(s)W(s) \rangle - \langle V \rangle \langle W \rangle].$$

The squared energy spread due to the action of the accelerating field only $\langle \Delta V^2 \rangle$ is calculated in a simple way as

$$\langle \Delta V^2 \rangle = \frac{1}{2}(1 - e^{-(k\sigma)^2})(1 - \cos(2\phi)e^{-(k\sigma)^2}).$$

The average squared energy spread $\langle \Delta W^2 \rangle$ caused by the wake fields only is

$$\langle \Delta W^2 \rangle = \frac{1}{Q}\int_{-\infty}^{+\infty} q(s)(W(s) - K_\sigma)^2 ds \tag{5}$$

We need two more additional integral parameters of the wake field for the calculation of the correlation expression $\langle V(s)W(s) \rangle$.

Introducing the Cosine-Fourier part

$$I_{cos} = \frac{1}{Q}\int_{-\infty}^{+\infty} q(s)W(s)(\cos(ks) - e^{-(k\sigma)^2/2})ds \tag{6}$$

and the Sine-Fourier part

$$I_{sin} = \frac{1}{Q}\int_{-\infty}^{+\infty} q(s)W(s)\sin(ks)ds \tag{7}$$

we finally obtain the RMS energy spread as

$$\sqrt{\langle \Delta U^2 \rangle} = \sqrt{U_0^2 \cdot \langle \Delta V^2 \rangle + Q^2 \cdot \langle \Delta W^2 \rangle + 2U_0 Q \cdot (I_{cos}\cos(\phi) - I_{sin}\sin(\phi))}. \tag{8}$$

Thus we need only four integral parameters of the wake field for the calculation of the RMS energy bunch spread in the accelerating structure: Loss factor K_σ (4), Average squared wake energy spread $\langle \Delta W^2 \rangle$ (5), Cosine-Fourier part I_{cos} (6) and Sine-Fourier part I_{sin} (7) .

5 Single bunch energy spread in the TESLA cryomodule

The integral parameters (in [V/pC]) of the wake fields of Gaussian bunches of different bunch lengths are given in Tab. 1. They are extracted from numerical time domain simulations of, at least, one complete TESLA cryomodule, including bellows and drift spaces (Fig. 1). In case of a 50μm long Gaussian bunch one cryomodule is not enough to reach the quasi periodic solution. For that reason a sequence of two cryomodules was simulated. The wake fields are given in the first and the second cryomodule.

σ/μm	K_σ/(V/pC)	I_{cos}/(V/pC)	I_{sin}/(V/pC)	$\sqrt{\langle \Delta W^2 \rangle}$/(V/pC)
1000	-88.70165	-0.5082225E-02	-1.067439	42.24653
700	-98.33152	-0.2461643E-02	-0.8492748	47.49361
400	-112.9101	-0.7956264E-03	-0.5698888	55.14657
300	-120.7278	-0.4647958E-03	-0.4562691	58.70800
250	-125.8536	-0.3754461E-03	-0.3914226	60.85590
50:I	-198.2546	-0.4340105E-04	-0.0960391	79.86720
50:II	-153.2351	-0.5752997E-05	-0.1107154	82.82798

Table 1: Integral parameters of the wake potentials of Gaussian bunches in the TESLA cryomodule.

The integral parameters are also calculated from the analytical approximation (Eq. 3) of the wake potentials. These values (Tab. 2) can be used to check the accuracy of the approximation.

σ/μm	K_σ/(V/pC)	I_{cos}/(V/pC)	I_{sin}/(V/pC)	$\sqrt{\langle \Delta W^2 \rangle}$/(V/pC)
700μm	-95.3	-2.15e-03	-0.859	47.837
400μm	-109.231	-6.418e-04	-0.57	55.147

Table 2: Integral parameters of the approximated wake fields (Eq. 3) of Gaussian bunches in the TESLA cryomodule.

In comparison to the parameters derived from the numerical simulation (Tab. 1), the analytically derived lossfactor is less than 5% lower, but the energy spread due to the wake fields only is well represented. This energy spread is approximately the energy spread of on crest acceleration ($\phi = 0$).

The single bunch energy spread according to Eq. 8 is calculated for different sets of TESLA parameters. The results for relative energy spread and energy gain are presented in the sections *TESLA-CDR* (5.1), *TESLA-500 high Luminosity* (5.2), *TESLA-800* (5.3), *TESLA-FEL* (5.4), *TTF-2* (5.5) and *TTF-FEL* (5.6) and illustrated with tables and plots for every parameter set.

The tables contain the relative energy spread at phase $\phi_0 = 0$ and the minimum energy spread at the optimum phase ϕ_{opt}. These parameters are given for different accelerating voltages within the reach of the respective project. The average energy gain $\langle U \rangle$, experienced by the bunch, is indicated for the phases ϕ_0 and ϕ_{opt}. The wavelength of the accelerating field is $\lambda = 230.768\text{mm}$.

5.1 TESLA-CDR ($\sigma = 700\mu\text{m}$, $Q = 5.8\text{nC}$)

Under the assumption, that the energy is high and the shape of the bunch is not affected, the wake fields are not a function of the particles energy. Depending on the peak accelerating voltage, different developments of the relative energy spread $\Delta U / \langle U \rangle$ and the relative average energy gain $\langle U \rangle / U_0$ as a function of the phase of injection can be found (Fig.9 and Fig.10 in case of a 700μm bunch with the charge $Q = 5.8nC$).

The higher the accelerating voltage, the lower is the influence of the wake fields on the energy spread for a given set of beam parameters (bunch length and charge). As a result the optimum phase ϕ_{opt} is closer to zero and the relative energy gain $\langle U \rangle / U_0$ is closer to one. The relative energy spread decreases with the increase of the accelerating voltage.

Obviously the relative energy spread has a unique minimum. Minimal energy spread and corresponding optimal phase for different accelerating voltages are presented in Tab. 3. For the design gradient of 25MV/m (corresponding to an energy gain of $U_0 = 200\text{MeV}$), stated in the CDR, the relative energy spread at $\phi = 0$ is $1.352 \cdot 10^{-3}$. The minimum achievable energy spread is $3.89 \cdot 10^{-4}$ at optimum phase $\phi_{opt} = -3.9^\circ$ and thus ≈ 3.5 times smaller than at $\phi = 0^\circ$.

Figure 11 demonstrates the energy gain as a function of the distance s to the bunch center for the design accelerating gradient of 25MV/m at $\phi = 0^\circ$ and $\phi_{opt} = -3.9^\circ$. Although the RMS energy spread is decreased, the difference between the maximum and the minimum energy gain along the bunch in the $-5\sigma, 5\sigma$ range is higher than at optimum phase.

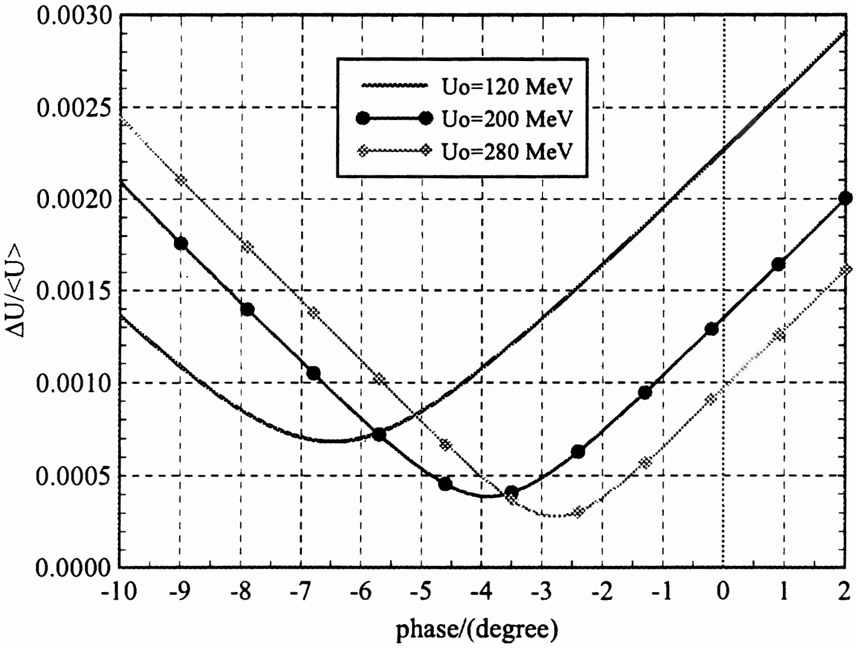

Figure 9: Relative energy spread due to a TESLA cryomodule (Bunch length $\sigma = 700\mu$m, Charge $Q = 5.8$nC).

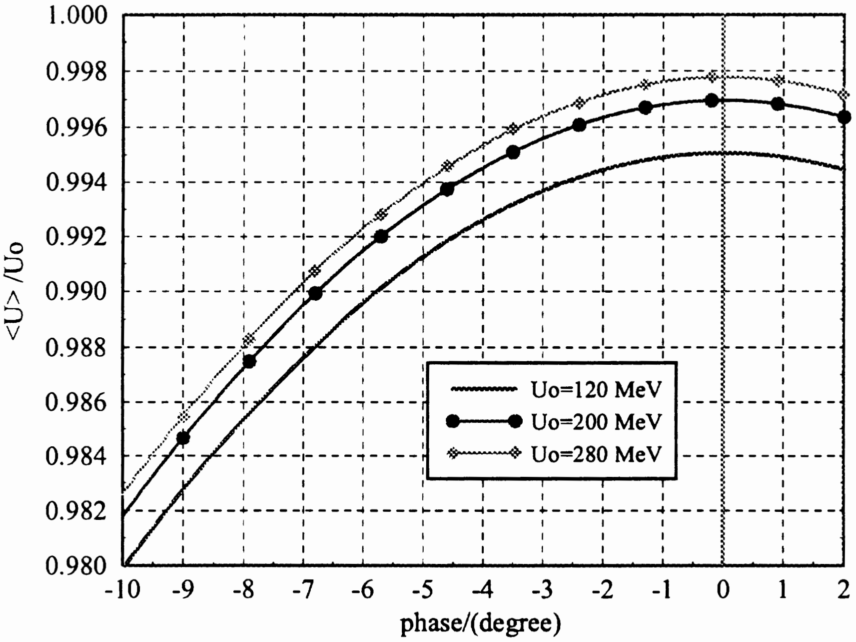

Figure 10: Relative energy gain due to a TESLA cryomodule (Bunch length $\sigma = 700\mu$m, Charge $Q = 5.8$nC).

U_0/MeV	Phase	$\langle U\rangle$/MeV,	$\Delta U/\langle U\rangle\cdot 1000$
160	ϕ =0°	159.401	1.695
	ϕ_{opt}=-4.9°	158.816	0.4953
180	ϕ =0°	179.397	1.5048
	ϕ_{opt}=-4.3°	178.89	0.4352
200	ϕ =0°	199.393	1.3532
	ϕ_{opt}=-3.9°	198.93	0.389
240	ϕ =0°	239.386	1.1273
	ϕ_{opt}=-3.2°	239.012	0.3245
280	ϕ =0°	279.379	0.9675
	ϕ_{opt}=-2.8°	279.045	0.283

Table 3: Energy gain and relative energy spread in a TESLA cryomodule in TESLA/CDR operation mode (Bunchlength σ = 700μm, Charge $Q = 5.8$nC). An energy gain of 200MeV corresponds to the design gradient of 25MV/m

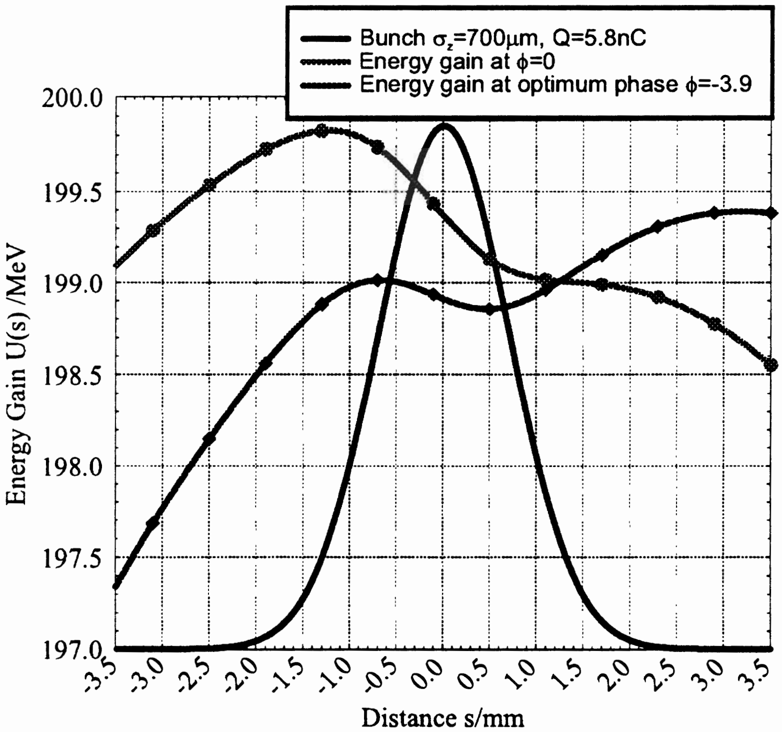

Figure 11: Energy gain of an electron inside a $\sigma = 700\mu$m bunch as a function of the distance to the bunch center in the TESLA cryomodule (Bunch charge $Q = 5,8$nC, peak accelerating voltage 200MV, optimal phase $\phi_{opt} = -3.9°$).

5.2 TESLA-500 high luminosity ($\sigma = 400\mu$m, $Q = 3.4$nC)

Tab. 4 shows minimal energy spread and corresponding optimal phase for different accelerating voltages for the TESLA-500 high luminosity upgrade. The bunch length is decreased to $\sigma = 400\mu$m and the bunch charge to $Q = 3.2$nC. The design gradient of the accelerating field stays the same as in the TESLA-CDR case. The energy spread at $\phi = 0$ increases to $1.5923 \cdot 10^{-3}$. The minimum achievable energy spread $4.707 \cdot 10^{-4}$ at optimum phase $\phi_{opt} = 8°$ is higher too. The decrease of the average energy gain at optimum phase is nearly 1%

U_0/MeV	Phase	$\langle U \rangle$/MeV,	$\Delta U / \langle U \rangle \cdot 1000$
160	ϕ =0°	159.336	1.9946
	ϕ_{opt}=-10°	156.905	0.6014
180	ϕ =0°	179.334	1.771
	ϕ_{opt}=-8.9°	177.167	0.5284
200	ϕ =0°	199.333	1.5923
	ϕ_{opt}=-8°	197.387	0.4707
240	ϕ =0°	239.331	1.3246
	ϕ_{opt}=-6.7°	237.692	0.3852
280	ϕ =0°	279.329	1.1336
	ϕ_{opt}=-5.7°	277.944	0.325

Table 4: Energy gain and relative energy spread in a TESLA cryomodule for the TESLA luminosity upgrade. (Bunchlength $\sigma = 400\mu$m, Charge $Q = 3.2$nC). An energy gain of 200MeV corresponds to the design gradient of 25MV/m

5.3 TESLA-800 ($\sigma = 300\mu$m, $Q = 2.24$ nC)

The upgrade of TESLA to a center of mass energy of 800GeV requires an increase of the gradient of the electric field in the accelerating structure up to 40MV/m (corresponding to $U_0 = 320$MeV).

For that reason the minimal energy spread and the corresponding optimal phase are given for high voltages only (Tab. 5).

The bunch length and bunch charge are decreased once more to $\sigma = 300\mu$m and to $Q = 2,24$nC respectively. The resulting energy spread is even lower than in the *TESLA-CDR* case.

U_0/MeV	Phase	$\langle U\rangle$/MeV,	$\Delta U/\langle U\rangle \cdot 1000$
280	ϕ =0°	279.72	0.4645
	ϕ_{opt}=-3.1°	279.311	0.1256
320	ϕ =0°	319.719	0.4061
	ϕ_{opt}=-2.7°	319.363	0.1086

Table 5: Energy gain and Energy spread in a TESLA Cryomodule for the TESLA 800 upgrade (Bunchlength $\sigma = 300\mu$m, Charge $Q = 2.24$nC).

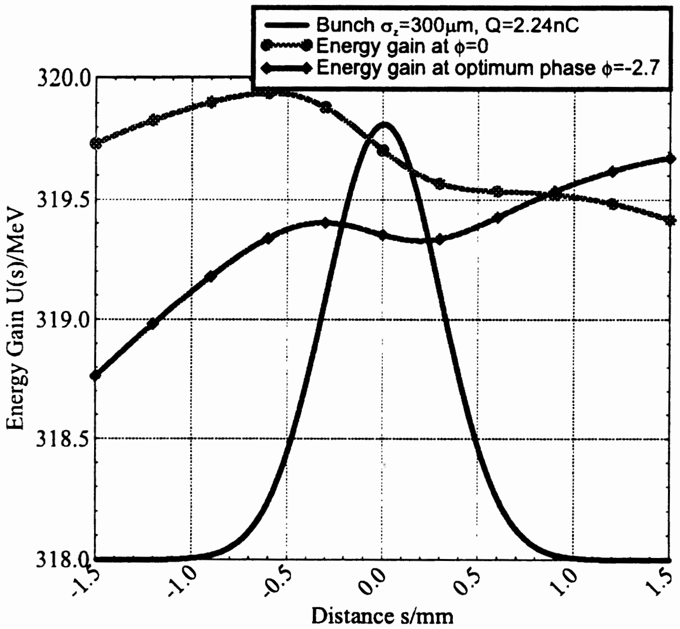

Figure 12: Energy gain of an electron inside a $\sigma = 300\mu$m bunch as a function of the distance to the bunch center in the TESLA cryomodule (Bunch charge $Q = 2.24$nC, peak accelerating voltage $U_0 = 320$MV, optimal phase $\phi_{opt} = -2.7°$).

5.4 TESLA-FEL ($\sigma = 50\mu$m, $Q = 1$nC)

For a $\sigma = 50\mu$m bunch, the relative energy spread $\Delta U/\langle U\rangle$ and the relative energy gain $\langle U\rangle/U_0$ as a function of the phase are shown in Fig.13 and Fig.14 for $U_0 = 200MeV$ and $Q = 1nC$. Since the steady state solution is not reached after one cryomodule, all numbers and figures are given for the first and the second cryomodule.

In the first cryomodule the minimum energy spread is more than twice as high as in the second module (Tab. 6). Since there is a large number of cryomodules in the part of the TESLA linear accelerator used for the FEL, the results of the second module are more relevant.

In the Conceptual Design Report an accelerating gradient of 18MV/m for FEL-operation is stated. This corresponds to $U_0 = 144MeV$. The on crest energy spread is then $5.549 \cdot 10^{-4}$ and $5.757 \cdot 10^{-4}$, the corrected $2.773 \cdot 10^{-4}$ and $1.195 \cdot 10^{-4}$ for the first and the second cryomodule respectively.

As the bunch length decreases, the wake fields become stronger and the optimum phase for minimal energy spread increases. For that reason the average energy gain at optimum phase is approximately 10% lower than at $\phi = 0$. The optimum phase offset ϕ_{opt} is higher for the second cryomodule than for the first, i.e. the decrease of the average energy gain at optimum phase is stronger. But it is not necessary to adjust the phase to the optimum value to reach the same energy spread as in the first module.

U_0/MeV	Phase	$\langle U\rangle$/MeV	$\Delta U/\langle U\rangle \cdot 1000$
120	ϕ =0°	119.802	0.6662
	ϕ_{opt}=-24°	109.427	0.3432
144	ϕ =0°	143.802	0.5549
	ϕ_{opt}=-20.2°	134.947	0.2773
160	ϕ =0°	159.802	0.4993
	ϕ_{opt}=-18.3°	151.71	0.2462
180	ϕ =0°	179.802	0.4437
	ϕ_{opt}=-16.3°	172.567	0.2161
200	ϕ =0°	199.802	0.3992
	ϕ_{opt}=-14.7°	193.255	0.1927

Table 6: Energy gain and relative energy spread in the first TESLA cryomodule in TESLA FEL operation mode (Bunchlength $\sigma = 50\mu$m, Charge $Q = 1$nC).

U_0/MeV	Phase	$\langle U\rangle$/MeV	$\Delta U/\langle U\rangle \cdot 1000$
120	ϕ =0°°	119.847	0.691
	ϕ_{opt}=-29.5°	104.29	0.1504
144	ϕ =0°	143.847	0.5757
	ϕ_{opt}=-24.3°	131.089	0.1195
160	ϕ =0°	159.846	0.5181
	ϕ_{opt}=-21.8°	148.404	0.1055
180	ϕ =0°	179.847	0.4605
	ϕ_{opt}=-19.3°	169.731	0.0921
200	ϕ =0°	199.847	0.4144
	ϕ_{opt}=-17.3°	190.799	0.0819

Table 7: Energy gain and relative energy spread in the second TESLA Cryomodule in TESLA FEL operation mode (Bunchlength $\sigma = 50\mu$m, Charge $Q = 1$nC).

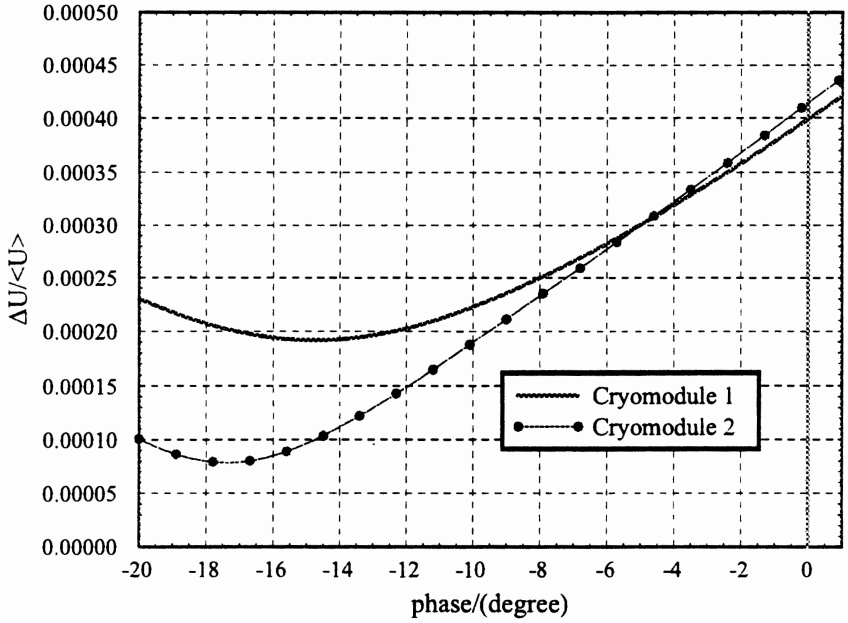

Figure 13: Relative energy spread in a TESLA cryomodule (Bunch length $\sigma = 50\mu\text{m}$, Charge $Q = 1\text{nC}$, $U_0 = 200\text{MeV}$).

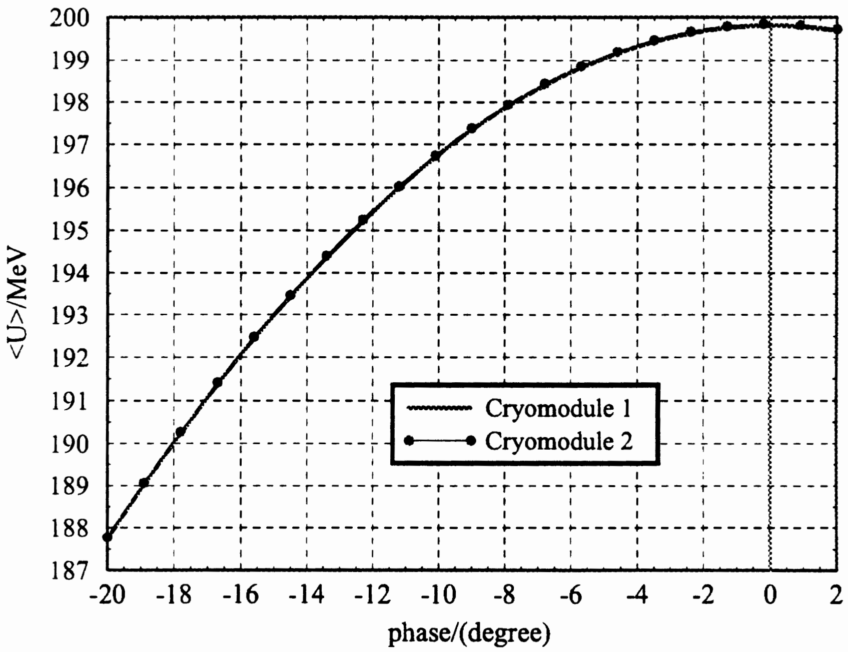

Figure 14: Energy gain in a TESLA cryomodule (Bunch length $\sigma = 50\mu\text{m}$, Charge $Q = 1\text{nC}$, $U_0 = 200\text{MeV}$).

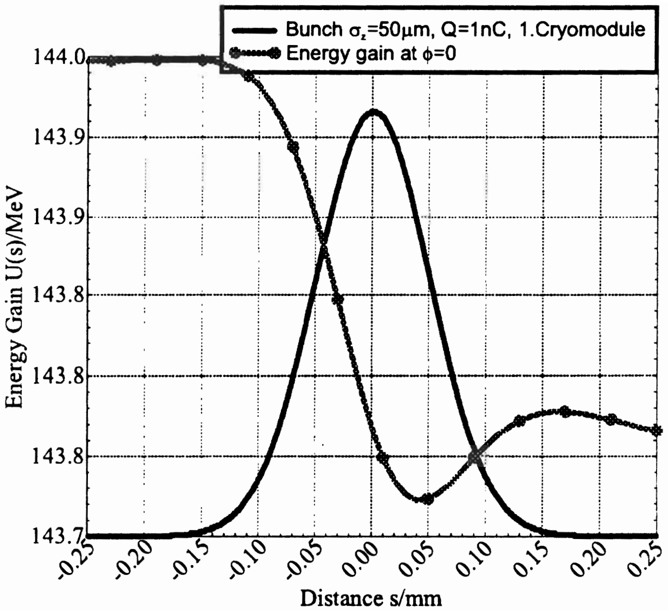

Figure 15: Energy gain of an electron as a function of the distance to the bunch center in the first TESLA cryomodule. (Bunch length σ = 50μm, charge Q = 1nC, U_0 = 144MeV and phase $\phi = 0°$).

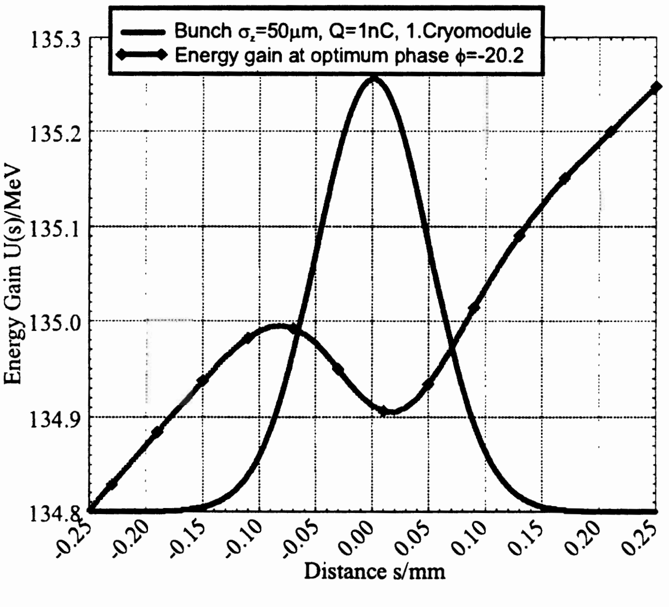

Figure 16: Energy gain of an electron as a function of the distance to the bunch center in the first TESLA cryomodule. (Bunch length σ = 50μm, charge Q = 1nC, U_0 = 144MeV and phase $\phi = -20.2°$).

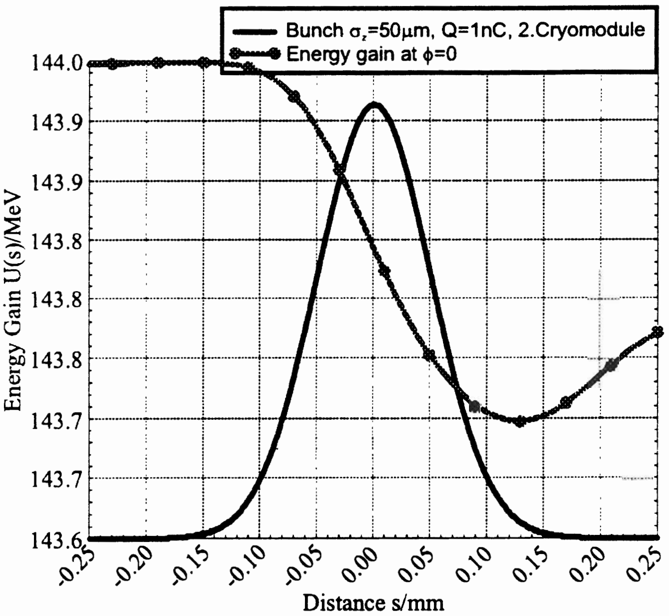

Figure 17: Energy gain of an electron as a function of the distance to the bunch center in the second TESLA cryomodule (Bunch length $\sigma = 50\mu$m, charge $Q = 1$nC, $U_0 = 144$MeV and phase $\phi = 0°$).

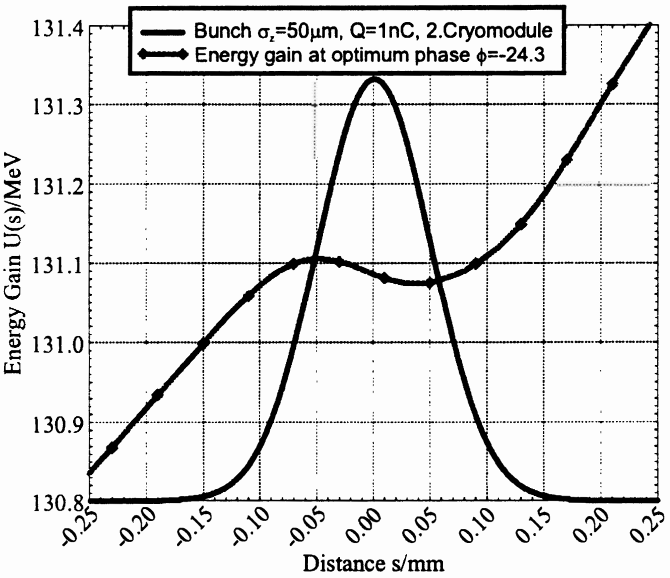

Figure 18: Energy gain of an electron as a function of the distance to the bunch center in the second TESLA cryomodule (Bunch length $\sigma = 50\mu$m, charge $Q = 1$nC, $U_0 = 144$MeV and phase $\phi = -24,3°$).

5.5 TTF-2 ($\sigma = 1000\mu$m, $Q = 8$nC)

Another set of beam parameters ($\sigma = 1000\mu$m, $Q = 8nC$) is used for the second stage of the TTF. The relative energy spread $\Delta U/\langle U\rangle$ and the energy gain $\langle U\rangle$ as a function of the injection phase are shown in Fig.19 and Fig.20 for $U_0 = 120$MeV. This corresponds to a gradient of the accelerating field of 15MV/m.

The minimal energy spread and the corresponding optimal phase for different accelerating voltages are displayed below (Tab. 8).

U_0/MeV	Phase	$\langle U\rangle$/MeV	$\Delta U/\langle U\rangle \cdot 1000$
100	ϕ =0°	99.253	3.3239
	ϕ_{opt}=-6.6°	98.591	1.0352
120	ϕ =0°	119.246	2.7613
	ϕ_{opt}=-5.5°	118.693	0.842
140	ϕ =0°	139.236	2.3627
	ϕ_{opt}=-4.7°	138.77	0.7129
160	ϕ =0°	159.231	2.0662
	ϕ_{opt}=-4.1°	158.822	0.6235
180	ϕ =0°	179.224	1.8378
	ϕ_{opt}=-3.7°	178.849	0.5603
200	ϕ =0	199.216	1.6568
	ϕ_{opt}=-3.3	198.885	0.5151

Table 8: Energy gain and relative energy spread in a TESLA Cryomodule for the TESLA 800 upgrade (Bunchlength $\sigma = 1000\mu$m, Charge $Q = 8$nC).

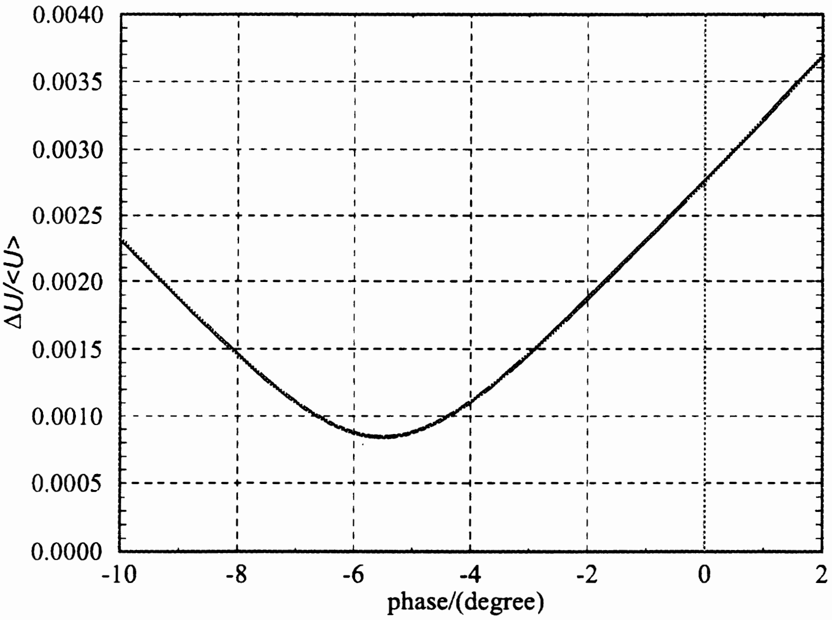

Figure 19: Relative energy spread in a TESLA cryomodule (bunch length $\sigma = 1\text{mm}$, Charge $Q = 8\text{nC}$, $U_0 = 120\text{MeV}$).

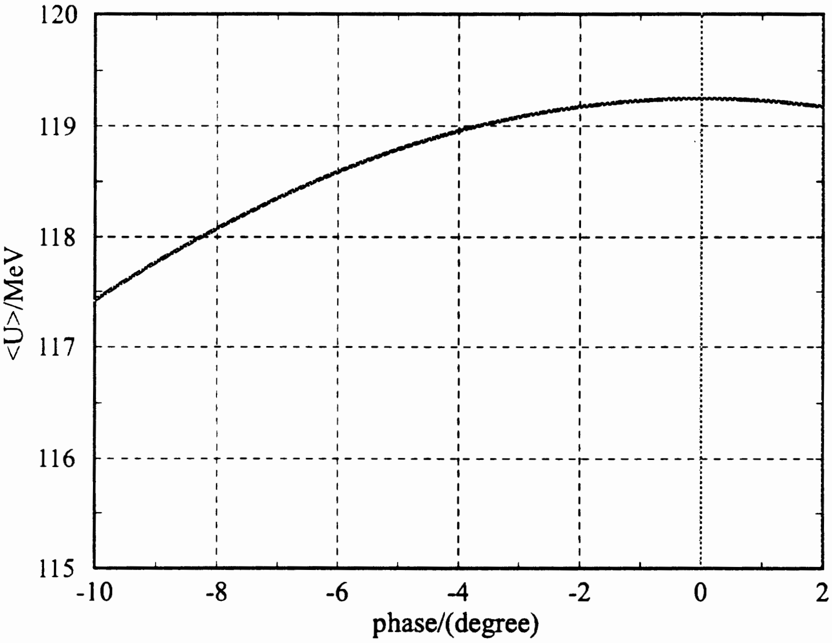

Figure 20: Energy gain in a TESLA cryomodule (bunch length $\sigma = 1\text{mm}$, Charge $Q = 8\text{nC}$, $U_0 = 120\text{MeV}$).

5.6 TTF-FEL ($\sigma = 250\mu$m, $Q = 1$nC)

The proof of principle experiment of the SASE-FEL at the TESLA Test Facility is one of the major milestones towards TESLA. The relative energy spread $\Delta U/\langle U\rangle$ and the energy gain $\langle U\rangle$ upon the phase degree for the design parameters $U_0 = 120$MeV, $\sigma = 250\mu$m and $Q = 1nC$, are shown in Fig.21 and Fig.22.

From the pictures we can see that there is an optimal phase, where the bunch gets the minimum energy spread. Energy distributions for the design parameters are displayed on Fig.23 for injection at $\phi = 0^\circ$ and at optimum phase ($\phi_{opt} = -4.1^\circ$).

Even after compensation, the energy spread has still linear dependence, at least for 60% of the particles. The compensation decreases the energy spread approximately 4 times.

Tab. 9 shows minimal energy spread at the optimal phase for 250μm 1nC bunches and for different accelerating voltages.

U_0/MeV	Phase	$\langle U\rangle$/MeV,	$\Delta U/\langle U\rangle \cdot 1000$
100	ϕ =0°	99.872	0.6032
	ϕ_{opt}=-4.9°	99.506	0.1655
120	ϕ =0°	119.871	0.5017
	ϕ_{opt}=-4.1°	119.564	0.1347
140	ϕ =0°	139.871	0.4293
	ϕ_{opt}=-3.5°	139.61	0.1128
160	ϕ =0°	159.87	0.3751
	ϕ_{opt}=-3°	159.651	0.0968
180	ϕ =0°	179.87	0.3293
	ϕ_{opt}=-2.7°	179.67	0.0841
200	ϕ =0°	199.87	0.2993
	ϕ_{opt}=-2.4°	199.694	0.0744

Table 9: Energy gain and relative energy spread in a TESLA cryomodule (bunch length $\sigma = 250\mu$m, charge $Q = 1$nC).

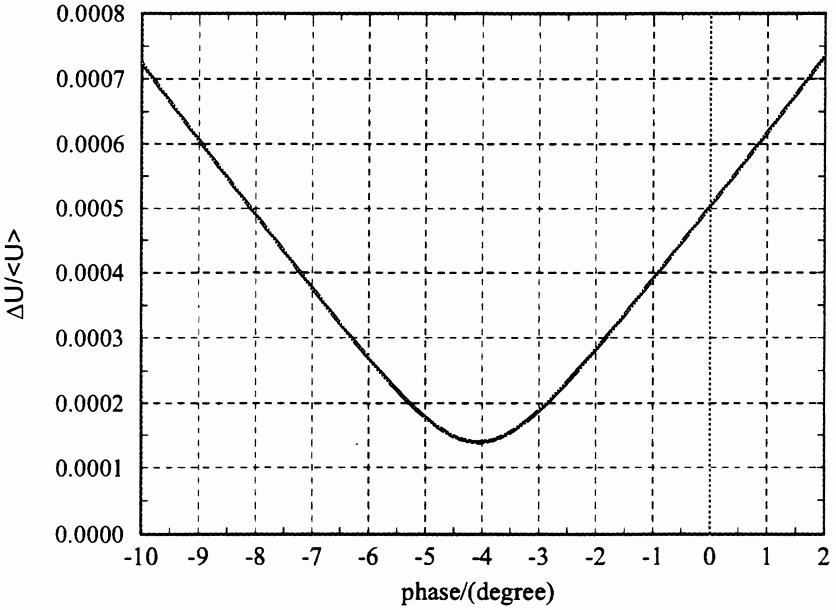

Figure 21: Relative energy spread in a TESLA cryomodule (bunch length $\sigma = 250\mu$m, Charge $Q = 1$nC, $U_0 = 120$MeV).

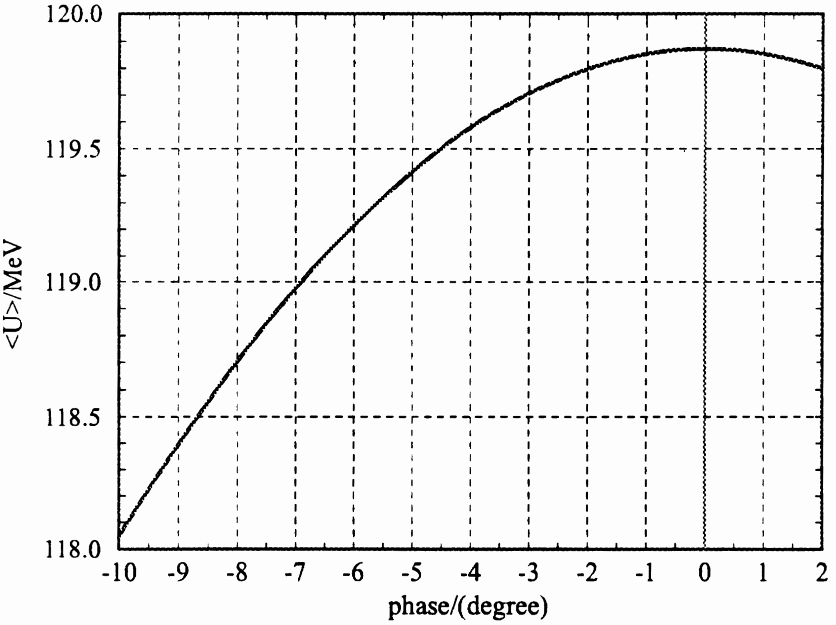

Figure 22: Energy gain in a TESLA cryomodule (bunch length $\sigma = 250\mu$m, Charge $Q = 1$nC, $U_0 = 120$MeV).

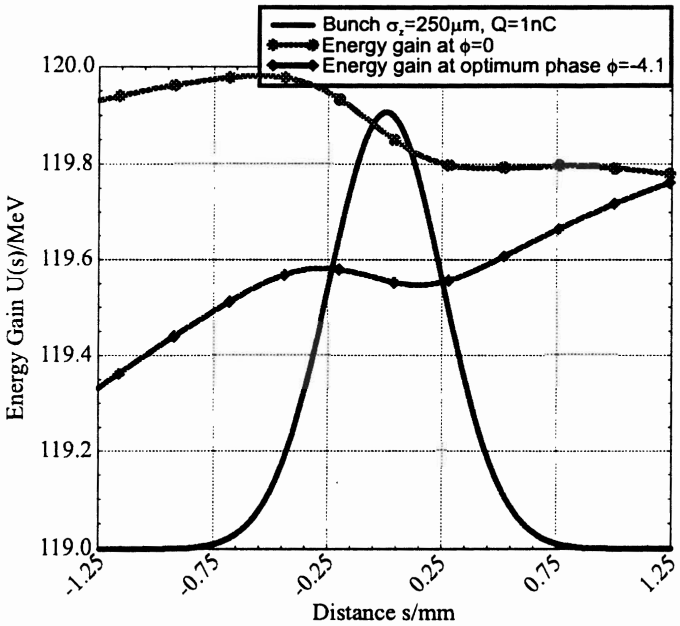

Figure 23: Energy gain of an electron as a function of the distance to the bunch center in the TESLA cryomodule (bunch length $\sigma = 250\mu$m, charge $Q = 1$nC, $U_0 = 120$MeV and optimal phase $\phi = -4.1°$).

6 Conclusion

In this paper wake field calculations of bunches of different length passing through TESLA accelerating cryomodules are presented. The simulation includes the bellows between single cavities and cryomodules, the different geometries of the end cells of the cavities and the drifts between cavities and cryomodules. It is shown, that for very short bunches ($\sigma = 50\mu$m) two consecutive cryomodules are not sufficient to reach the steady state solution. The wake fields of different bunches follow a common curvature within a range of $300\mu\text{m} < s < 20\text{mm}$.

An approximation of the wake function is given for beam dynamics calculations. The wake function approximates the common curvature too. The approximation is compared to the numerical results. A good agreement for all discussed parameter sets is found within the range of validity.

A formula for the calculation of the RMS energy spread due to wake fields and accelerating voltage is derived. It is shown, that the knowledge of 4 parameters is sufficient to describe the energy spread including the correlation between wake fields and accelerating voltage.

This formula and the results of the numerical simulations are applied to different parameter sets discussed for TESLA and the TTF. There is a unique minimum of the energy spread depending on the phase of the accelerating voltage. By choosing the optimum phase the energy spread can be reduced up to 5 times. The results are presented in a number of Figures and Tables and can serve for further beam dynamics considerations.

7 Acknowledgements

The authors want to thank R. Brinkmann and J. Rossbach for their interest in this work and their support.

References

[1] "Conceptual Design of a 500 GeV e^+e^- Linear Collider with Integrated X-ray Laser Facility", DESY 1997-048, ECFA 1997-182, DESY, Hamburg, 1997.

[2] R. Brinkmann (for the TESLA Collaboration), "Linear Collider Projects at DESY", Proceedings of the EPAC-98, pp.53-57, Stockholm, Sweden, 1998.

[3] "TESLA Test Facility- Conceptual Design Report", TESLA 95-01, DESY, Hamburg, 1995.

[4] "A VUV Free Electron Laser at the TESLA Test Facility at DESY", TESLA-FEL 95-03, DESY, Hamburg, 1995.

[5] The MAFIA collaboration "User Guide", CST GmbH, Darmstadt, Germany

[6] A.Novokhatski, M.Timm, T.Weiland. -Transition Dynamics of the Wake Fields of Ultra Short Bunches.- Proceed. of ICAP '98, Monterey 1998.

[7] A.Novokhatski and A.Mosnier, "Short Bunch Wake Potentials for a Chain of TESLA Cavities", DAPNIA/SEA-96-08, 1996.

[8] K. Bane, M. Timm, and T. Weiland, "The Short Range Wake Fields in the SBLC," *Proceedings of the PAC'97*, pp. 515–517, 1997.